American Journal of Pathology, Vol. 166, No. 6, June 2005

Gastrointestinal, Hepatobiliary and Pancreatic Pathology

Absence of CCR6 Inhibits CD4$^+$ Regulatory T-Cell Development and M-Cell Formation inside Peyer's Patches

Andreas Lügering,* Martin Floer,* Sabine Westphal,* Christian Maaser,* Thomas W. Spahn,* M. Alexander Schmidt,† Wolfram Domschke,* Ifor R. Williams,‡ and Torsten Kucharzik*

From the Departments of Medicine B and Infectiology,† University of Münster, Münster, Germany; and the Departments of Pathology and Laboratory Medicine and of Dermatology,‡ Emory University School of Medicine, Atlanta, Georgia*

The chemokine Mip3α is specifically expressed by the follicle-associated epithelia (FAE) covering intestinal Peyer's patches (PPs) and is the only known chemokine ligand for the chemokine receptor CCR6. Although CCR6-deficient mice are known to have a perturbed intestinal immune system, little is known about the specific impact of this interaction for Peyer's patch formation. To elucidate the effect of Mip3α on PP lymphocyte development, we used a CCR6/enhanced green fluorescent protein (EGFP) knock-in mouse model and analyzed lymphocyte development by immunohistochemistry and flow cytometry. PPs of CCR6$^{-/-}$ mice were significantly size-reduced with a proportional loss of B cells and T cells, whereas T-cell subsets were disturbed with a decreased CD4/CD8 ratio paralleled with a loss of regulatory CD4$^+$ CD45Rb^{low} T cells. The analysis of cytokine production by CCR6-expressing cells could demonstrate that CCR6 is involved in the regulation of cytokine secretion such as interleukin-12 by dendritic cells. Quantification of UEA-1$^+$ cells inside the FAE showed reduced M-cell numbers in CCR6-deficient mice. These results suggest that the interaction of CCR6 with its ligand Mip3α is important for immune responses generated inside the PPs, particularly for the generation of regulatory CD4$^+$ T cells residing inside PPs and for the formation of M cells. ***(Am J Pathol 2005, 166:1647–1654)***

Chemokines constitute a family of structurally related chemotactic cytokines that direct the migration of leukocytes under physiological and inflammatory conditions. Furthermore, several chemokines have been shown to be involved in physiological functions such as angiogenesis, tumor growth, or metastasis.[1]

Generally, chemokines activate G-protein-coupled receptors on their target cells through binding to their corresponding chemokine receptors. Although most chemokine receptors have several different chemokine ligands, others only bind to a single receptor. In mice, Mip3α has been shown to be selectively secreted by the follicle-associated epithelium (FAE) covering Peyer's patches (PPs) of the intestine. In 1996, three different groups identified the CCL20 receptor CCR6 in dendritic cells based on migration experiments and calcium mobilization assays and showed that CCL20 was not able to bind to other known chemokine receptors.[2–4]

Recently, we generated a CCR6-EGFP knock-in mouse model and thereby demonstrated the expression of CCR6 in myeloid dendritic cells (DCs), most B cells, parts of CD4 T cells, and a small fraction of CD8 T cells.[5] In addition, we could identify CCR6 expression in lineage-marker-negative, c-kit$^+$ extrathymic T-cell precursors specifically inside cryptopatches, the supposed side of extrathymic IEL generation.[6] The latter is likely to be related to the expansion of extrathymic intraepithelial lymphocytes (IEL) seen in all CCR6-knockout models described so far.

Initially, CCR6 was supposed to be involved in the migration process of myeloid DCs toward the subepithelial dome region of PPs, whereas other types of CCR6-expressing cells were not affected.[7,8] However, a detailed analysis of several independently generated CCR6 knockout (KO) models including our CCR6 knock-in con-

Supported by grants from the Deutsche Forschungsgemeinschaft (LU816/2-1 to A.L.), the Innovative Medizinische Forschung (LÜ110318 to A.L.), the National Institutes of Health (grant DK-64730 to I.R.W.)

Accepted for publication February 10, 2005.

Address reprint requests to Andreas Lügering, M.D., Department of Medicine B, University of Münster, Albert-Schweitzer-Strasse 33, D-48129 Münster, Germany. E-mail: lugerin@uni-muenster.de.

struct could identify $CD11c^+CD11b^+$ myeloid DCs in the dome area of all mice, indicating that CCR6 is not solely necessary for myeloid DC migration inside PPs.[9]

M cells (membranous or microfold) are specialized epithelial cells found inside the FAE covering the Peyer's patches and are involved in antigen sampling.[10] M cells show a deep invagination of the basolateral membrane that contains lymphocytes and phagocytic leukocytes. The origin of intestinal M cells still remains controversial:[11] initially, it was assumed that M cells derive from undifferentiated precursors inside the crypts adjacent to the dome. It could be demonstrated that a subpopulation of crypt cells seems to be predetermined as M cells before acquiring the corresponding morphological features.[12] However, recent studies could show that human intestinal epithelial cells may be converted into functional M cells *in vitro* by interaction with Peyer's patch-derived lymphocytes.[13]

Recently, Jump and Levine[14] demonstrated that PPs contain distinct CD4 T-cell subsets including a significantly higher number of regulatory $CD4^+$ T cells supposed to have recently been exposed to antigens when compared with mesenteric lymph node or spleen cells. This particular subset specifically produces interleukin (IL)-10 and suppresses T-cell proliferation *in vitro* on stimulation through TCR/CD3 and therefore might mediate natural tolerance to antigens taken up from the lumen of the intestine.

In this study, we used EGFP-CCR6 knock-in/knockout mice to identify the physiological role of the Mip3α-CCR6 interaction for the development of Peyer's patches and M cells. We could show that the deletion of CCR6 specifically reduces the size of PPs and alters CD4 T-cell subsets inside PPs with a specific loss of regulatory $CD62L^+CD45Rb^{low}$ CD4 T cells, whereas the recruitment and localization of CCR6-expressing cells toward PPs and the subepithelial dome area is not affected. In addition, dendritic cells from CCR6 KO mice secrete a substantially greater amount of IL-12. The imbalance of the PP immune system in CCR6 KO mice also affects M-cell formation inside the FAE. These results suggest that CCR6 is primarily not responsible for the migration of leukocytes under physiological conditions but instead regulates PP CD4 T-cell and M-cell development.

Materials and Methods

Mice

The gene-targeting strategy used to generate CCR6 EGFP knock-in mice was described in a previous report.[5] The homozygous CCR6-deficient mice used for these studies were back-crossed four times to C57BL/6. CCR6 KO mice and heterozygous CCR6-deficient mice shared the same background. When genotyping of the individual offspring was required, a three-primer polymerase chain reaction (PCR) method was used. Comparisons of CCR6-deficient and KO mice were made using heterozygous and homozygous knockout mice that were typically littermates between 6 and 8 weeks of age.

Preparation of Peyer's Patch Cell Suspensions

Peyer's patch lymphocytes were prepared by a standard method with minor modifications. Briefly, Peyer's patches were removed; washed with a cold solution of Ca^{2+} and Mg^{2+}-free Hanks' balanced salt solution, 10 mmol/L HEPES, 25 mmol/L $NaHCO_3$, and 2% (v/v) fetal bovine serum, pH 7.2; and minced between histological slides. To further isolate the PP lymphocytes, the tissue was incubated with 100 U/ml collagenase D (Roche, Grenzach-Wyhlen, Germany) and 5 U/ml DNase (Sigma, St. Louis, MO) for 30 minutes at 37°C in complete RPMI media. The cells released into the supernatant were isolated from the interface of a 44%/66% Percoll gradient (Amersham, Ismaning, Germany), centrifuged for 30 minutes at 600 $\times$ *g*, and washed in cold phosphate-buffered saline (PBS). Cells from spleen and mesenteric lymph nodes were isolated in parallel.

Generation of Bone Marrow-Derived Dendritic Cells

Bone marrow-derived dendritic cells were isolated as described previously.[15] Briefly, bone marrow was isolated from femur and tibia and erythrocytes were lysed. The remaining cells were plated at the density of 10^6 per milliliter in 6-well plates in RPMI (Hyclone, Logan, UT) supplemented with 10% fetal bovine serum (Hyclone) and containing 10 ng/ml of murine GM-CSF and 1 ng/ml of murine IL-4 (Peprotech, Rocky Hill, NJ). The cells were incubated at 37°C with 5% CO_2. After 2 days of culture, the cells were gently washed and replaced with RPMI-10 containing the same concentration of GM-CSF and IL-4 for an additional 5 days.

Cytokine Enzyme-Linked Immunosorbent Assay (ELISA)

Day-7 bone marrow-derived DCs were treated with lipopolysaccharide (LPS) at a final concentration of 1 μg/ml. The supernatants were collected 48 hours after stimulation, and an IL-10 and IL-12p40 enzyme-linked immunosorbent assay (BD Biosciences, Heidelberg, Germany) was performed according to the manufacturer's instructions. Spleen cells were plated on mouse anti-CD3 T-cell activation plates (BD Biosciences) and cultured for 72 hours. The supernatants were collected, and an interferon-γ and IL-2 ELISA (BD Biosciences) was performed according to the manufacturer's instructions. All experimental groups were tested in triplicates.

Antibodies and Flow Cytometry

Monoclonal antibodies used to stain cell suspensions were purchased from BD Pharmingen, Heidelberg, Germany (biotin-anti-CD3 (145-2C11), PE-anti-CD4 (RM4-5), biotin-anti-CD4 (RM4-5), APC-anti-CD8α (53-6.7), PE-anti-CD11c (HL3), PE-anti-CD19 (1D3), and PE-anti-CD45Rb) and eBioscience (San Diego, CA) (APC-anti CD62L and PE-

anti-CD69). Binding of biotinylated antibodies was detected with streptavidin conjugated to CyChrome (Pharmingen, Heidelberg, Germany). Antibodies were diluted in PBS containing 0.2% bovine serum albumin and 0.02% NaN_3 for 30 minutes on ice. Data on antibody-stained cell suspensions was acquired on a dual laser FACScan flow cytometer (Becton Dickinson), and the results were analyzed using Cell Quest 3.3 (Becton Dickinson). Cell populations were gated on the basis of forward and side scatter to allow selection of the viable lymphocytes.

Immunofluorescence Staining

For detection of *in situ* EGFP fluorescence, mice were perfused with 3% paraformaldehyde followed by 10% sucrose before embedding of the tissue in OCT as described elsewhere.[6] Six-micrometer frozen sections were cut with a cryostat. $CCR6^+$ cells were detected by means of their EGFP expression; control stainings were done in parallel on tissue from wild-type mice to exclude autofluorescence signals. All controls were negative. PE-anti CD4, PE-anti-B220, and biotin-anti-CD11c monoclonal antibodies (in combination with a streptavidin conjugated to PacificBlue (Molecular Probes, Eugene, OR), 1 μg/ml) were used to detect cellular localization inside PPs using 5 μg/ml of the primary antibody. DAPI (4,6-diamino-2-phenylindole, Sigma) was used as nuclear counterstain. Double- and triple-color fluorescence images were acquired using a Zeiss microscope (Carl Zeiss AG, Oberkochen, Germany). M cells inside the FAE were identified by UEA-1 (Sigma) staining as described elsewhere.[16] Mip3α expression was detected on acetone-fixed tissue sections using a monoclonal biotinylated antibody to murine Mip3α (0.1 μg/ml final concentration; R&D Systems, Wiesbaden, Germany) followed by tyramide signal amplification system with streptavidin-peroxidase and fluorescein isothiocyanate-tyramide (PerkinElmer Life Sciences, Boston, MA).

Electron Microscopy

Tissue specimens were rinsed with PBS, immediately fixed in 2.5% glutaraldehyde (Sigma) in PBS overnight, postfixed in 1% osmium tetroxide for 2 hours, rinsed in PBS, and dehydrated through a graded series of ethanol (Sigma), which was finally replaced with propylene oxide (Sigma). Afterward, the tissue was embedded in Epon (Serva, Heidelberg, Germany) and hardened for 48 hours at 65°C. After identification of the area of interest on semithin sections stained with toluidine blue, Peyer's patches were cut with diamond knives on an ultra-microtome (0.05 μm) and mounted on noncoated mesh grids. The sections were contrasted with 5% uranyl acetate and 0.1% lead citrate (Sigma) and examined with a Philips CM10 electron microscope.

Reverse Transcriptase-PCR Analysis

Whole PP tissue RNA was isolated using TRIzol reagent (Life Technologies, Gaithersburg, MD) according to the instructions of the manufacturer, and 2 μg of total RNA was transcribed to cDNA. The PCR reaction was performed using 1 μl of the cDNA product produced by the reverse transcription reaction using cycle conditions and primer pairs described elsewhere.[17] Nontranscribed samples were used as control. All controls were negative.

Statistics

Results are generally expressed as the mean $\pm$ SD, unless stated otherwise. The statistical significance of differences between groups was evaluated by Student's *t*-test. A *P* value of less than 0.05 was considered to be statistically significant.

Results

CCR6-Deficient Mice Have Size-Reduced Peyer's Patches

The unique chemokine ligand for the chemokine receptor CCR6, Mip3α, is specifically expressed by the FAE covering Peyer's patches. Earlier studies on CCR6-deficient mice came to controversial results concerning the size of Peyer's patches, whereas both studies determined regular numbers (8 to 10/small intestine) when compared with wild-type control mice. We were able to identify similar numbers of PPs in our KO mice as well when compared with wild-type control mice or heterozygous littermates; however, the PPs from CCR6 KO mice were significantly size-reduced, as determined by the total number of cells recovered after lymphocyte isolation (3.9×10^6 versus 1.9×10^6 per mouse; $P < 0.05$; Figure 1A).

Cellular Composition of PPs in CCR6-Deficient Mice

Because CCR6-deficient mice revealed significantly size-reduced PPs, we determined the cellular composition of PPs, mesenteric lymph nodes, and spleen regarding B, T, and dendritic cells by 4-color flow cytometry using antibodies to B220, CD3, and CD11c, respectively. In parallel, we examined the proportion of CCR6-expressing cells in Peyer's patches from CCR6 KO and heterozygous knock-in mice by means of EGFP-expression to determine whether the functional loss of the CCR6 protein results in a reduced proportion of CCR6-expressing cells.

As demonstrated in Figure 1B, CCR6 KO mice show a proportional loss of both B and T cells inside PPs because no difference could be determined regarding the relative proportions of B220 (52.8 versus 51.2%; $P > 0.1$) and CD3 (44.7 versus 48.9%; $P > 0.1$), suggesting regular B- and T-cell subsets inside PPs. Additional subanalysis of B cells such as for the surface expression of immunoglobulins were not able to identify significant differences either (data not shown). In contrast, CCR6-deficient mice show a slightly increased number of $CD11c^+$ cells.

The additional analysis of CCR6-expressing subfractions inside the B- and T-lymphocyte fraction was not able to identify a significant loss of CCR6-expressing cells from

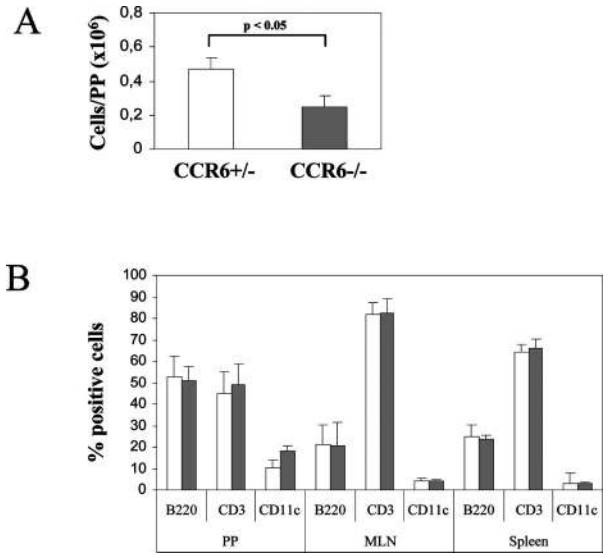

Figure 1. Cellular composition of organized lymphoid tissue of CCR6 KO mice. **A:** Total cells of Peyer's patches of CCR6-deficient mice (**filled bars**) and heterozygous controls (**open bars**) showed a significantly decrease of PP lymphocytes in CCR6 KO mice (4.7 ± 0.07 versus $2.5 \pm 0.06 \times 10^5$cells/PP; $P < 0.05$). To further elucidate the absence of distinct lymphocyte subsets, the cellular composition of Peyer's patches, mesenteric lymph nodes, and spleens from CCR6 KO mice and heterozygous controls was analyzed by flow cytometry using antibodies to T cells, B cells, and dendritic cells (**B**). Whereas a modestly increased number of CD11c cells could be found inside size-reduced PPs from CCR6 KO mice, no difference could be observed in the overall distribution of T and B cells (all P values >0.1). Additional analysis of mesenteric lymph nodes and spleens from both types of mice did not show any difference. The mean and standard deviations are shown for five mice per group that have been analyzed independently.

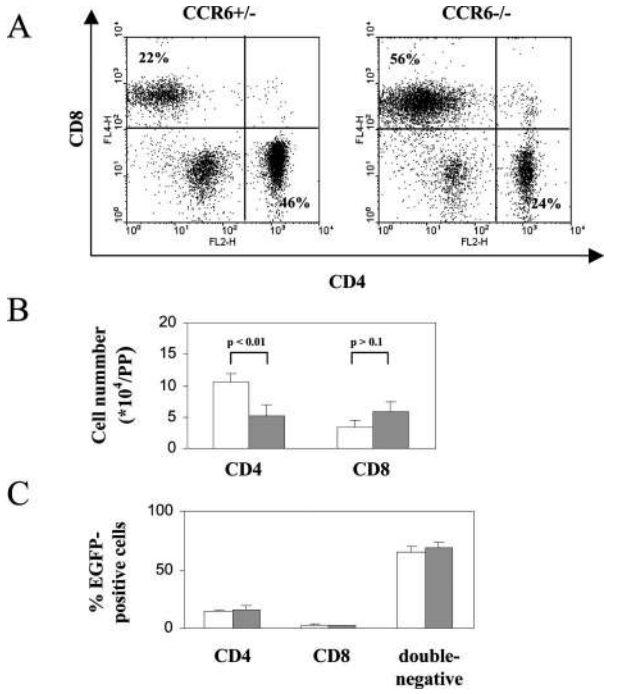

Figure 2. Analysis of T-cell subsets from CCR6 KO Peyer's patches. T cells recovered from Peyer's patches were stained with antibodies to CD3, CD4, and CD8 from CCR6 KO and heterozygous control mice. **A:** A typical set of data acquired from five independently analyzed mice per group (gated for $CD3^+$ lymphocytes). **B:** Compared with heterozygous controls (**open bars**), PPs from CCR6 KO mice (**filled bars**) contain significantly fewer CD4 T cells and similar absolute numbers of CD8 T cells. **C:** In contrast, the relative amount of CCR6-expressing cells as determined by EGFP expression remains constant in all subsets (P not significant in all subsets).

CCR6 KO Peyer's patches (data not shown). Similar analysis from leukocytes recovered from mesenteric lymph nodes or spleen did not show any significant differences regarding the total number of cells or of the cellular subsets.

CCR6 Affects Formation of Peyer's Patch Regulatory CD4 T-Cell Development

Because earlier studies showed a significant influence of the CCR6 chemokine receptor on T-cell development, we also asked whether PPs from CCR6 KO mice might display different T-cell subsets. We therefore analyzed the $CD3^+$ cellular subsets from PPs in more detail. As shown in Figure 2, CCR6 KO mice have significantly fewer $CD4^+$ T cells inside their PPs ($10.6 \times 10^4 \pm 2.2$ versus $3.4 \times 10^4 \pm 1.7$ per PP; $P < 0.01$), whereas the $CD8^+$ T cells remain constant in absolute numbers ($5.1 \times 10^4 \pm 1.7$ versus $5.9 \times 10^4 \pm 1.5$ per PP; $P > 0.1$). In addition, PPs from CCR6 KO mice also harbor significantly fewer $CD3^+CD4^-CD8^-$ lymphocytes (9.9 versus 18.1%). We also determined the proportion of CCR6-expressing cells in all subsets. Whereas both major CCR6-expressing fractions ($CD4^+CD8^-$ and $CD4^-CD8^-$) did not show any significant difference in their proportion of CCR6-expressing cells, a mild increase of CCR6-expressing cells was observed in the $CD8^+$ subset (4.2 versus 2.5%); however, the amount of positive cells appeared to be limited in both types of mice. In contrast, no comparable differences could be determined inside mesenteric lymph nodes or spleen. These results suggest that CCR6 affects extrathymic T-cell lymphopoiesis supposed to occur within PPs, whereas it does not affect T-cell recruitment into PP or systemic T-cell development.

Recent studies suggest that PPs contain a specific $CD4^+CD62L^-CD45Rb^{low}$ regulatory T-cell population expressing high levels of IL-10 on stimulation through the CD3/TCR complex.[14] We therefore stained CD4 T cells from CCR6-deficient mice and heterozygous control mice for CD62L, CD45Rb, and CD69. As shown in Figure 3, heterozygous control mice contain a significant amount of $CD62L^-CD45Rb^{low}$ cells, corresponding to earlier reports, whereas a significantly reduced population was found in CCR6-deficient mice (32.3 versus 10.0%; $P < 0.005$). In parallel, more $CD4^+CD62L^-$ T cells recovered from PPs of CCR6-deficient mice expressed high levels of CD69 when compared with age-matched control mice (data not shown).

Distribution of CD4 T Cells inside PPs from CCR6-Deficient Mice

To further elucidate the effect of CCR6 on $CD4^+$ T cells, we stained PPs from heterozygous control mice and CCR6 KO mice. To characterize the anatomy of a complete follicle and to avoid misinterpretations due to differences in projection, we performed serial sections 50 μm apart in each PP. As shown in Figure 4A, control mice

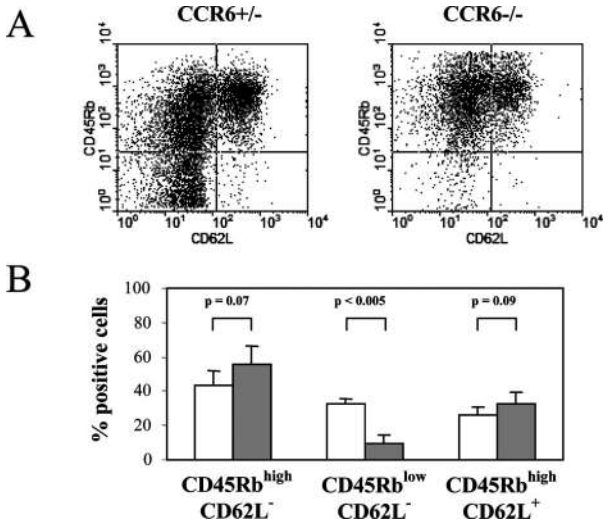

Figure 3. Loss of regulatory $CD4^+$ T cells from CCR6 KO Peyer's patches. Lymphocytes were isolated from PPs of CCR6 KO and heterozygous control mice. CD4 T-cell subsets within the PPs were identified by flow cytometry using antibodies to CD62L and CD45Rb. **A:** A typical four-color fluorescence-activated cell sorter (FACS)- analysis gated on $CD4^+$ lymphocytes with a significant loss of $CD45Rb^{low}$ cells from PPs of CCR6 KO mice ($10.0 \pm 4.4\%$) compared with heterozygous control mice ($32.3 \pm 3\%$; $P < 0.01$). **B:** The statistical data represent four pools of two mice from each genotype analyzed independently.

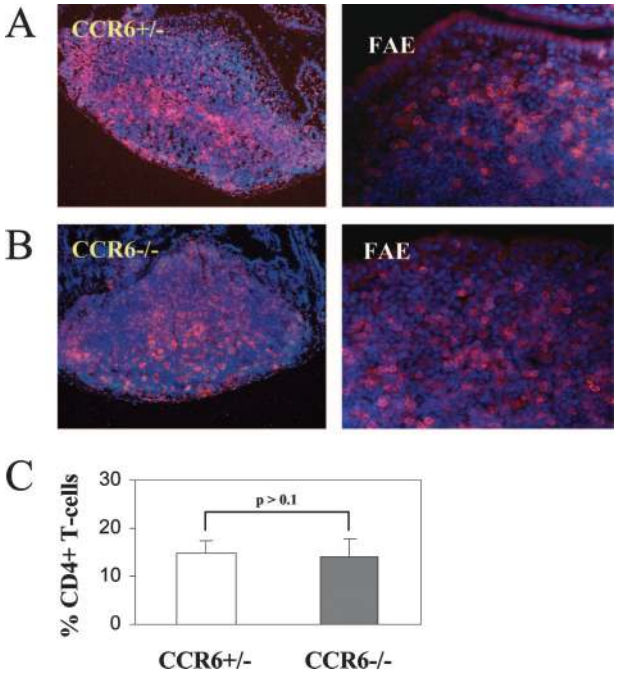

Figure 4. Localization of CD4 T cells. To evaluate the distribution of CD4 T cells, serial sections of PPs were done 50 μm apart including the whole follicle. In general, PPs of CCR6 KO mice appeared different because they are smaller and contain fewer follicles when compared with wild-type controls as described previously.[7] **A:** CD4 immunostaining of PPs from control mice exhibited $CD4^+$ T cells (Alexa 546, red) predominantly inside the interfollicular region as well as inside the follicle between the germinal center and the subepithelial dome area. **B:** In CCR6 KO mice, the distribution pattern appears to be more diffuse, but the preferential localization of CD4 T cells remains constant. **C:** In addition, almost equivalent numbers of $CD4^+$ cells are found within the SED region of wild-type and CCR6 KO mice (representative for 12 PPs obtained from three different mice from each genotype).

showed $CD4^+$ T cells predominantly inside the interfollicular region as well as inside the follicle between the germinal center and the subepithelial dome area. Even though PPs appear significantly reduced in size, CCR6 KO mice showed a similar distribution of the CD4 T-cell subset (Figure 4B), indicating that the loss of CCR6 is not inducing a major architectural change in the morphology of PPs. Similarly, the quantification of $CD4^+$ cells inside the SED region did not reveal a significant loss of CD4 T cells from the area where Mip3α is expressed (Figure 4C).

CCR6 Does Not Affect Cellular Migration toward the FAE

The selective expression of the only CCR6 ligand, Mip3α, by the follicle-associated epithelia covering Peyer's patches (Figure 5A) suggests that the Mip3α-CCR6 interaction influences the migration of CCR6-expressing cells toward the subepithelial dome (SED) region. In fact, in both of the first two models of CCR6-deficient mice, a selective deficiency of $CD11c^+CD11b^+$ myeloid DC recruitment toward the SED in the absence of CCR6 was observed. However, a recent report that summarized several independently generated models identified $CD11c^+CD11b^+$ myeloid DCs in the SED area. We therefore asked whether CCR6-deficient mice might show differences in their SED region based on expression of the knocked-in EGFP gene product in CCR6-sufficient heterozygous and CCR6-deficient homozygous KO mice. PPs from both types of mice were perfusion-fixed and stained for CD11c and B220 in parallel. As shown in Figure 5, CCR6 KO mice show a regular distribution of PP cellular subsets, and EGFP-positive cells are similarly distributed inside the PPs of CCR6-deficient mice compared with heterozygous control mice including the presence of $B220^+$ B cells as well as $CD11c^+$ dendritic cells in the SED area, indicating that CCR6 does not affect specific cellular migration toward the FAE.

Analysis of CCR6-Dependent Cytokine Expression in Vivo *and* in Vitro

To evaluate whether leukocytes from PPs of CCR6 KO mice might exhibit a gross difference regarding their cytokine profile, we first analyzed the expression of tumor necrosis factor-α, IL-4, transforming growth factor-β, and IL-10 inside PPs of wild-type and CCR6 KO mice by reverse transcriptase-PCR. As shown in Figure 6A, we were able to detect significantly lower levels of IL-10 in PPs of CCR6 KO mice, potentially indicating a loss of $CD4^+CD45Rb^{low}$ cells as shown above known to be a major source of IL-10. However, all other cytokines examined did not show any major differences.

To identify a CCR6-dependent cytokine expression in distinct cellular subsets, we determined cytokine secretion of stimulated bone marrow-derived DCs (BmDCs) expressing high levels of CCR6 (75%, data not shown) and CD3-stimulated splenocytes. In the absence of a functional receptor, BmDCs secreted significantly higher levels of IL-12 after stimulation with LPS, whereas secretion of IL-10 was not affected (Figure 6B). Similarly, CD3-stimulated spleen cells of CCR6-deficient mice also produced significantly

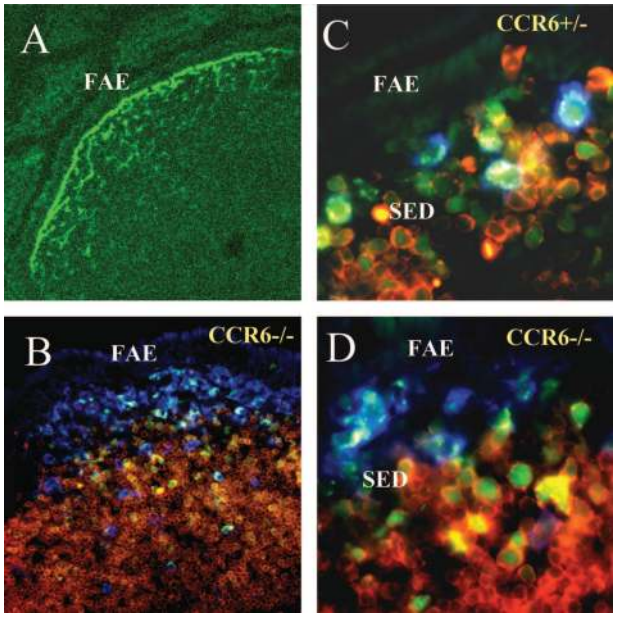

Figure 5. Localization of EGFP-expressing cells. **A:** Immunofluorescent characterization of Mip3α expression (green) revealed a selective basolateral secretion by the FAE of Peyer's patches. The relevance of receptor expression by leukocytes for localization inside the subepithelial dome area (SED) was analyzed by triple-color immunohistochemistry. In CCR6-deficient EGFP knock-in mice, B cells (B220-PE, red) and dendritic cells (CD11c, Pacific blue) are regularly distributed, and EGFP-expressing cells are found underneath the FAE (**B**, ×20; **D**, ×100), showing no difference when compared with heterozygous control mice (**C**, ×100).

higher levels of interferon-γ and IL-2 when compared with wild-type control (Figure 6C). The data indicate that CCR6 is capable of regulating cytokine expression by receptor-expressing cells such as DC or T cells.

CCR6-Deficient Mice Exhibit Reduced Numbers of M Cells

M cells are specialized cells inside the follicle-associated epithelia involved in antigen sampling across the intestinal barrier. Even though the origin of M cells has not been completely characterized, it seems likely that they convert from regular epithelial cells within the FAE by interacting with the mononuclear cells inside PPs. However, the exact mechanism still remains to be elucidated. Because Mip3α is selectively expressed by the FAE and disruption of its only ligand CCR6 induces distinct alterations in the lymphocyte composition inside the PPs, we asked whether the inhibition of Mip3α-CCR6 interaction influences M-cell formation. M-cell numbers were determined inside the FAE from heterozygous control mice and CCR6 KO mice by staining with the lectin UEA-1 known to specifically bind murine M cells. We could demonstrate that CCR6-deficient mice reveal a significantly reduced number of M cells when compared with heterozygous littermates (Figure 7). In addition, we evaluated the appearance of M cells inside the FAE of CCR6 KO mice by transmission electron microscopy (TEM). Only a limited number of epithelial cells were found that showed distinct M-cell features such as irregular microvilli or an M-cell pocket (data not shown).

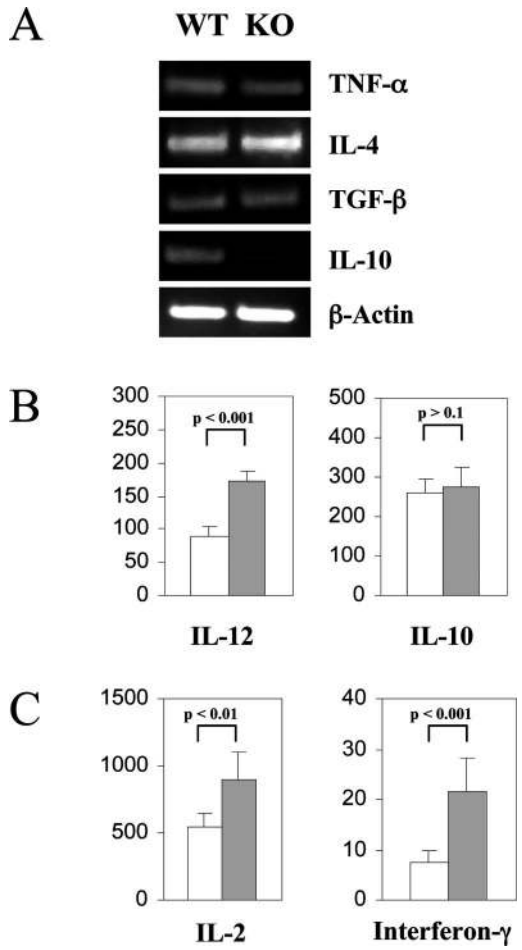

Figure 6. CCR6 regulates DC and T-cell cytokine expression. Cytokine expression of PP leukocytes from CCR6-deficient mice was compared with wild-type controls by reverse transcriptase-PCR. RNA was isolated from whole PPs, and expression of tumor necrosis factor-α, IL-4, transforming growth factor-β, and IL-10 was analyzed. **A:** The reduced expression of IL-10 inside PPs of CCR6-deficient mice, whereas no changes were obvious for all other cytokines evaluated. The data are representative data from three mice each group. **B:** IL-12 and IL-10 secretion of BmDCs after LPS stimulation were analyzed by ELISA. CCR6-deficient BmDCs (**filled bars**) secrete significantly higher amounts of IL-12 (90.2 ± 13.5 ng/ml versus 171.8 ± 15.8 ng/ml; $P < 0.001$) compared with controls (**open bars**), whereas no differences were detected for IL-10 (260 ± 35 pg/ml versus 273 ± 53 pg/ml; $P > 0.1$). Splenocytes from the same mice were stimulated by plate-bound anti-CD3 and interferon-γ and IL-2 measured after 48 hours by ELISA (**C**) showing significant increased expression of interferon-γ (7.6 ± 2.1 ng/ml versus 21.6 ± 6.6 ng/ml; $P < 0.001$) as well as IL-2 (540 ± 100 pg/ml versus 890 ± 200 pg/ml; $P < 0.01$) in CCR6-deficient mice. The data are representative for four independent experiments including one to two mice per group.

Discussion

Chemokines and chemokine receptors play an integral role in the homeostasis of various lymphoid organs *in vivo* under physiological and inflammatory conditions. Whereas some chemokines act as housekeeping chemokines and are expressed by a broad variety of different tissues, others serve as tissue-selective chemokines involved in organ-specific homing. Mip3α is selectively expressed by the FAE covering PPs inside the intestine. The FAE contains M cells serving as the portal of entry for intestinal antigens and pathogens.[18]

In the current study, we focused on the effect of CCR6 disruption on the development of PP and M-cell formation.

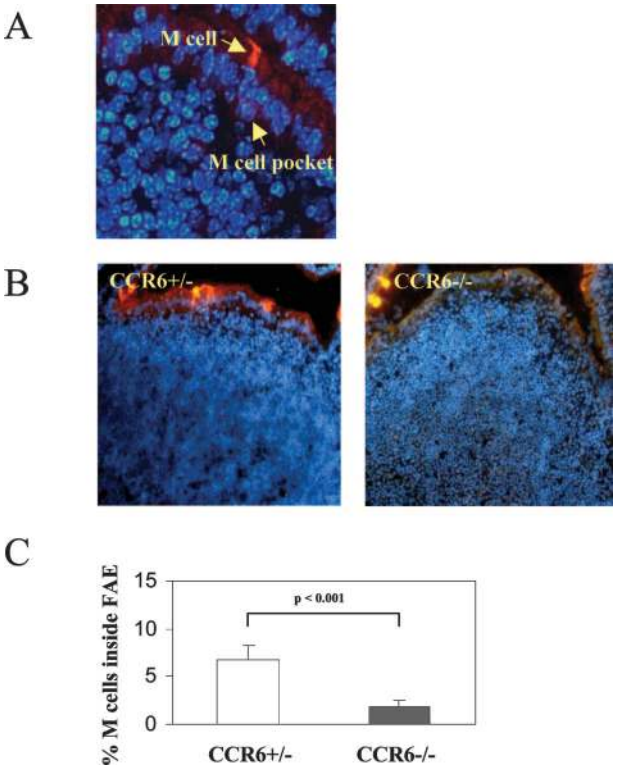

Figure 7. Reduced number of M cells within the FAE of CCR6-deficient mice. M cells were identified by staining with the rhodamine-conjugated UEA-1 lectin known to specifically label M cells inside the murine FAE. **A:** A typical staining of an M cell (red) that contains several leukocytes in its basolateral pocket. **B:** To analyze the effect of CCR6 on M-cell formation, multiple sections of Peyer's patch of heterozygous control and CCR6-deficient mice from multiple litters were stained. The total number of follicle-associated epithelial cells was quantified by nuclear counterstain (DAPI, blue). Whereas control mice (**open bars**) contain 6.8% M cells within the FAE, CCR6 KO mice (**filled bars**) exhibited a significantly reduced number (1.8%) of UEA-1$^+$ cells inside FAE ($P < 0.001$; **C**). The data represent the mean and SEM from 10 sections of six randomly selected Peyer's patches of five mice representing each genotype.

We found that CD4 T cells are specifically diminished inside PPs, whereas MLN or systemic lymphoid organs are not affected. More interestingly, the disruption of CCR6 did not induce a loss of EGFP-expressing cells from PPs or the SED region in our knock-in construct, suggesting that CCR6 is not primarily inducing migration toward the FAE. In contrast, cytokine secretion studies could prove that CCR6 is capable of regulating cytokine secretion in receptor-expressing cells, particularly the secretion of IL-12 by dendritic cells. Finally, we could demonstrate that the conversion of M cells from follicle-associated epithelial cells is inhibited by loss of CCR6. Therefore, it seems to be likely that the formation of M cells is dependent on lympho-epithelial interactions mediated by Mip3α and CCR6.

Multiple studies have been carried out to characterize the bioactivity of Mip3α on various sources of leukocytes expressing the chemokine receptor CCR6.[19] Whereas several *in vitro*-generated types of DCs and CD4$^+$ and CD8$^+$ T cells as well as B cells show CCR6 mRNA and protein expression and reveal chemotaxis to Mip3α *in vitro*, no obvious chemotactic effect could be determined so far *in vivo*. Initially, two groups independently described a specific lack of CD11c$^+$CD11b$^+$ myeloid DCs from the SED region of CCR6-deficient mice,[7,8] but it has been shown recently that this observation was not consistent when comparing most of the CCR6 KO models simultaneously.[9] In our system, we were able to track CCR6-expressing leukocytes *in vivo* by means of EGFP expression and could demonstrate by flow cytometry and immunohistochemistry that CCR6 KO mice contain similar amounts and types of EGFP-expressing cells in their PPs and SED region when compared with CCR6-sufficient heterozygous EGFP knock-in control mice. In addition, earlier studies by our group could demonstrate that intestinal cryptopatches harbor similar amounts of CCR6-expressing IEL precursors as control mice.[6] It therefore seems to be likely that Mip3α does not exert chemotactic activity on CCR6-expressing leukocytes under physiological conditions. However, it cannot be ruled out that CCR6-mediated chemotactic effects occur under distinct inflammatory conditions or when secondary stimuli are present. It is also conceivable that other chemokine receptor-ligand interactions might partly compensate the loss of CCR6.

Although CCR6 is present on CD8$^+$ T cells, several *in vivo* observations such as contact hypersensitivity reactions[7] or delayed allograft rejection (unpublished observations) have demonstrated that the deletion of CCR6 is rather functional on CD4$^+$ T cells. In our study, we found that the deletion of CCR6 specifically influences the CD4 T-cell subset within the Peyer's patch, whereas mesenteric lymph nodes and spleen cells were not affected. However, previous reports on CCR6 mice showed conflicting results regarding the influence of CCR6 on PP formation. Whereas Cook et al[8] found regular shaped PPs in CCR6 KO mice, Varona et al[7] reported significantly size-reduced PPs in their CCR6 KO model corresponding to our observations. We found moderate changes of PPs in the initial mixed genetic background, whereas size reduction as well as specific changes in CD4 T cells became more obvious after further backcrossing toward C57BL/6. In addition, exposure to distinct dietary antigens and different bacterial loads are factors known to influence the PP phenotype that might account for differences in the published models.

In an oncostatin M overexpression model where massive thymus-independent T-cell development and major expansion of the memory T-cell pool occurs, Louis et al[20] recently found that Mip3α is the first molecule found to increase the proliferation of memory phenotype CD4$^+$ T cells. No corresponding effects were found on CD8$^+$ T cells. We could also demonstrate that CD4$^+$CD62L$^-$CD45Rb^{low} regulatory T cells specifically residing inside PPs are predominantly lacking inside PPs from CCR6 KO mice, suggesting that Mip3α secreted by the FAE potentially enhances the formation of this particular subset. Of note is also the high expression of CCR6 by CD4$^-$CD8$^-$ cells within PPs where extrathymic precursors are supposed to reside,[21] whereas CCR6 expression is absent in double-negative T-cell precursors in the thymus (unpublished data). These data support the view that expression of CCR6 by immature T cells is not a general phenomenon associated with all forms of T-cell differentiation, but it is instead a specialized adaptation for development of the extrathymic T-cell populations.

Intriguingly, we were able to show that BmDCs of CCR6 KO mice secrete significantly higher levels of IL-12 after *in vitro* stimulation, whereas IL-10 secretion was not affected. IL-12 is known to induce interferon-γ secretion, induces T helper 1-cell differentiation, and forms a link between innate resistance and adaptive immune system.[22] We were able to find an increased interferon-γ as well as IL-2 secretion of splenic T cells as well as an enhanced lytic activity of intraepithelial lymphocytes against the intestinal nematode *Heligmosomoides polygyrus* (unpublished observations). However, it remains to be elucidated, eg, by conditional knockouts, whether this phenomenon contributes to the CCR6 KO phenotype *in vivo*.

Although several studies have examined the ontogenesis of M cells, their origin still remains obscure. Basically, two major routes to M cells have been discussed. First, it was hypothesized that M cells might constitute a different cell lineage as epithelial cells showing distinct M-cell features in dome-associated crypts were identified.[16] However, multiple studies could demonstrate that immunological conditions in the FAE are more likely to be responsible for M-cell induction. Recently, Kerneis et al[13] were able to convert epithelial cells into M cells *in vitro* by interaction with PP lymphocytes. Multiple studies demonstrated that different cellular subsets and also tumor cell lines such as Raji B cells are effective in converting epithelial cells into M cells.[23] However, the exact interaction necessary for the conversion process remains unclear. In our study, we were able to demonstrate a decreased proportion of M cells within the FAE of CCR6-deficient mice, suggesting a role of this chemokine ligand for the conversion of follicle-associated epithelial cells into M cells. Recently, we could also demonstrate that an increased M-cell conversion occurs under inflammatory conditions in rats associated with an increased appearance of CD4 T cells within the M-cell pocket.[24] It is therefore conceivable that M-cell conversion is associated with lympho-epithelial interactions involving CCR6-expressing CD4 T cells and Mip3α-secreting epithelia. Further studies are needed to investigate whether M cells outside the FAE are associated with similar events.

References

1. Zlotnik A, Yoshie O: Chemokines: a new classification system and their role in immunity. Immunity 2000, 12:121–127
2. Greaves DR, Wang W, Dairaghi DJ, Dieu MC, Saint-Vis B, Franz-Bacon K, Rossi D, Caux C, McClanahan T, Gordon S, Zlotnik A, Schall TJ: CCR6, a CC chemokine receptor that interacts with macrophage inflammatory protein 3alpha and is highly expressed in human dendritic cells. J Exp Med 1997, 186:837–844
3. Baba M, Imai T, Nishimura M, Kakizaki M, Takagi S, Hieshima K, Nomiyama H, Yoshie O: Identification of CCR6, the specific receptor for a novel lymphocyte-directed CC chemokine LARC. J Biol Chem 1997, 272:14893–14898
4. Power CA, Church DJ, Meyer A, Alouani S, Proudfoot AE, Clark-Lewis I, Sozzani S, Mantovani A, Wells TN: Cloning and characterization of a specific receptor for the novel CC chemokine MIP-3alpha from lung dendritic cells. J Exp Med 1997, 186:825–835
5. Kucharzik T, Hudson JT III, Waikel RL, Martin WD, Williams IR: CCR6 expression distinguishes mouse myeloid and lymphoid dendritic cell subsets: demonstration using a CCR6 EGFP knock-in mouse. Eur J Immunol 2002, 32:104–112
6. Lugering A, Kucharzik T, Soler D, Picarella D, Hudson JT III, Williams IR: Lymphoid precursors in intestinal cryptopatches express CCR6 and undergo dysregulated development in the absence of CCR6. J Immunol 2003, 171:2208–2215
7. Varona R, Villares R, Carramolino L, Goya I, Zaballos A, Gutierrez J, Torres M, Martinez AC, Marquez G: CCR6-deficient mice have impaired leukocyte homeostasis and altered contact hypersensitivity and delayed-type hypersensitivity responses. J Clin Invest 2001, 107:R37–R45
8. Cook DN, Prosser DM, Forster R, Zhang J, Kuklin NA, Abbondanzo SJ, Niu XD, Chen SC, Manfra DJ, Wiekowski MT, Sullivan LM, Smith SR, Greenberg HB, Narula SK, Lipp M, Lira SA: CCR6 mediates dendritic cell localization, lymphocyte homeostasis, and immune responses in mucosal tissue. Immunity 2000, 12:495–503
9. Zhao X, Sato A, Dela Cruz CS, Linehan M, Luegering A, Kucharzik T, Shirakawa AK, Marquez G, Farber JM, Williams I, Iwasaki A: CCL9 is secreted by the follicle-associated epithelium and recruits dome region Peyer's patch CD11b+ dendritic cells. J Immunol 2003, 171:2797–2803
10. Neutra MR: Current concepts in mucosal immunity. V. Role of M cells in transepithelial transport of antigens and pathogens to the mucosal immune system. Am J Physiol 1998, 274:G785–G791
11. Nicoletti C: Unsolved mysteries of intestinal M cells. Gut 2000, 47:735–739
12. Gebert A, Posselt W: Glycoconjugate expression defines the origin and differentiation pathway of intestinal M-cells. J Histochem Cytochem 1997, 45:1341–1350
13. Kerneis S, Bogdanova A, Kraehenbuhl JP, Pringault E: Conversion by Peyer's patch lymphocytes of human enterocytes into M cells that transport bacteria. Science 1997, 277:949–952
14. Jump RL, Levine AD: Murine Peyer's patches favor development of an IL-10-secreting, regulatory T cell population. J Immunol 2002, 168:6113–6119
15. Nguyen LT, Radhakrishnan S, Ciric B, Tamada K, Shin T, Pardoll DM, Chen L, Rodriguez M, Pease LR: Cross-linking the B7 family molecule B7-DC directly activates immune functions of dendritic cells. J Exp Med 2002, 196:1393–1398
16. Clark MA, Jepson MA, Simmons NL, Booth TA, Hirst BH: Differential expression of lectin-binding sites defines mouse intestinal M-cells. J Histochem Cytochem 1993, 41:1679–1687
17. Andres PG, Beck PL, Mizoguchi E, Mizoguchi A, Bhan AK, Dawson T, Kuziel WA, Maeda N, MacDermott RP, Podolsky DK, Reinecker HC: Mice with a selective deletion of the CC chemokine receptors 5 or 2 are protected from dextran sodium sulfate-mediated colitis: lack of CC chemokine receptor 5 expression results in a NK1.1+ lymphocyte-associated Th2-type immune response in the intestine. J Immunol 2000, 164:6303–6312
18. Iwasaki A, Kelsall BL: Localization of distinct Peyer's patch dendritic cell subsets and their recruitment by chemokines macrophage inflammatory protein (MIP)-3alpha, MIP-3beta, and secondary lymphoid organ chemokine. J Exp Med 2000, 191:1381–1394
19. Schutyser E, Struyf S, Van Damme J: The CC chemokine CCL20 and its receptor CCR6. Cytokine Growth Factor Rev 2003, 14:409–426
20. Louis I, Dulude G, Corneau S, Brochu S, Boileau C, Meunier C, Cote C, Labrecque N, Perreault C: Changes in the lymph node microenvironment induced by oncostatin M. Blood 2003, 102:1397–1404
21. Guy-Grand D, Azogui O, Celli S, Darche S, Nussenzweig MC, Kourilsky P, Vassalli P: Extrathymic T cell lymphopoiesis: ontogeny and contribution to gut intraepithelial lymphocytes in athymic and euthymic mice. J Exp Med 2003, 197:333–341
22. Trinchieri G: Interleukin-12 and the regulation of innate resistance and adaptive immunity. Nat Rev Immunol 2003, 3:133–146
23. Kerneis S, Caliot E, Stubbe H, Bogdanova A, Kraehenbuhl J, Pringault E: Molecular studies of the intestinal mucosal barrier physiopathology using cocultures of epithelial and immune cells: a technical update. Microbes Infect 2000, 2:1119–1124
24. Lugering A, Floer M, Lugering N, Cichon C, Schmidt MA, Domschke W, Kucharzik T: Characterization of M cell formation and associated mononuclear cells during indomethacin-induced intestinal inflammation. Clin Exp Immunol 2004, 136:232–238